Microchimica Acta (2018) 185: 102
https://doi.org/10.1007/s00604-017-2622-4

ORIGINAL PAPER

Determination of the activity of alkaline phosphatase by using nanoclusters composed of flower-like cobalt oxyhydroxide and copper nanoclusters as fluorescent probes

Hai-Bo Wang[1] · Yang Li[1] · Ying Chen[1] · Zi-Ping Zhang[2] · Tian Gan[3] · Yan-Ming Liu[1,3]

Received: 12 December 2017 / Accepted: 15 December 2017 / Published online: 10 January 2018

Abstract

The authors describe a sensitive fluorometric method for the determination of the activity of alkaline phosphatase (ALP). It is based on the use of a composite prepared consisting of flower-like cobalt oxyhydroxide (CoOOH) and copper nanoclusters (CuNCs). On formation of the CuNC-CoOOH aggregates, the fluorescence of the CuNCs is quenched by the CoOOH sheets. If, however, the CoOOH sheets are reduced to Co(II) ions in the presence of ascorbic acid (AA), fluorescence recovers. AA is formed in-situ by hydrolysis of the substrate ascorbic acid 2-phosphate (AA2P) as catalyzed by ALP. Thus, the ALP activity can be detected indirectly by kinetic monitoring of the increase in fluorescence, best at excitation/emission wavelengths of 335/410 nm. The assay allows ALP to be determined in 0.5 to 150 mU·mL^{-1} activity range and with a 0.1 mU·mL^{-1} detection limit. The method was successfully applied to the determination of ALP activity in (spiked) human serum samples. The assay has attractive features in being of the off-on type and immune against false positive results.

Keywords CoOOH sheets · CuNC-CoOOH aggregates · Fluorometric assay · Alkaline phosphatase activity detection · Biosensor · Fluorescence recovery · Cobalt(II) · Ascorbic acid 2-phosphate

Introduction

As a new kind of 2D layered nanomaterials, transition metal oxides (TMOs) and their derivatives, such as MnO_2 and CoOOH, have attracted increasing research interest owing to their excellent physical and chemical properties [1, 2]. CoOOH sheets, an emerging kind of transition metal oxides derivatives, possess a broad and strong absorption band around 410 nm, making CoOOH sheets be used as a broad-spectrum quencher [2]. In the past few years, CoOOH sheets have been utilized as fluorescence quenchers to construct fluorescence resonance energy transfer (FRET) bio/chemical sensing platforms [2–6]. Tang's group found that CoOOH nanoflakes have oxidizing capability and can react with ascorbic acid (AA) instantaneously [2]. On the basis of the finding, they have reported CoOOH-modified persistent luminescence nanoparticles for the fluorescence imaging assay of AA in living cells and in vivo. Cen et al. have exploited a nanosystem for the monitoring of AA in human plasma by using CoOOH sheets-modified fluorescent upconversion nanoparticles [5]. Meng et al. have utilized two-photon nanoparticles

Electronic supplementary material The online version of this article (https://doi.org/10.1007/s00604-017-2622-4) contains supplementary material, which is available to authorized users.

✉ Hai-Bo Wang
wanghaibohn@163.com

✉ Tian Gan
gantianxynu@163.com

[1] College of Chemistry and Chemical Engineering, Henan Province Key Laboratory of Utilization of Non-metallic Mineral in the Sourth of Henan, Xinyang Normal University, Xinyang 464000, People's Republic of China

[2] College of Life Science, Yantai University, Yantai 264005, People's Republic of China

[3] Institute for Conservation and Utilization of Agro-bioresources in Dabie Mountains, Xinyang Normal University, Xinyang 464000, People's Republic of China

and CoOOH nanoflakes to report a turn-on strategy for fluorescent determination and imaging of AA in living cells and tissues [6]. However, the preparation process of these fluorescent nanomaterials is relatively complicated and harsh. Chu's group discovered that CoOOH nanoflakes exhibited different adsorption ability between single stranded-DNA (ss-DNA) and double stranded-DNA (ds-DNA), which resulted in the fluorescence signal of dye-labeled ss-DNA was significantly quenched by CoOOH nanoflakes, while ds-DNA still had strong fluorescence emission [7]. On the basis of the phenomenon, they have constructed a CoOOH nanoflakes based fluorescent bioassay platform for the detection of protein thrombin, T4 polynucleotide kinase activity and its inhibition screening [7, 8]. Nevertheless, the exploration of CoOOH nanomaterials for bio/chemical assay is still at early stage [9].

Alkaline phosphatase (ALP) as an enzyme widely present in mammalian tissues and organs, catalyzes the hydrolysis and dephosphorylation process on various substrates including nucleic acids, proteins, and small molecules [10]. ALP also plays vital roles in cellular regulation (such as cell cycle, growth, apoptosis), and signal transduction processes. As a result, the ALP activity is often regarded as an important biomarker in some diseases diagnosis. The normal level of ALP in human serum is 40–190 $U{\cdot}L^{-1}$ (for adults), whereas the ALP level of children and pregnant women is more than 500 $U{\cdot}L^{-1}$ [11]. The abnormal levels of serum ALP is closely related to some diseases, such as hepatitis, diabetes, liver dysfunction, breast and prostate cancer, and so on [12–15]. Therefore, sensitive and selective determination the ALP content is of significant importance.

Various methods have been reported to determinate the ALP activity, including colorimetric assay [16, 17], chemiluminescence [18], surface enhanced Raman scattering [19], and electrochemical methods [20]. Although some of these methods exhibit high sensitivity, most of them suffer from laborious or complicated synthetic and prepared procedures. Due to their high sensitivity, cost effectiveness, simplicity, and convenience, fluorescent methods have drawn considerable attention [21–25]. A great deal of fluorescent assays have been reported for detecting the ALP activity on the basis of quantum dots (QDs) [26], conjugated polyelectrolytes [27], and organic fluorophores [28]. However, these strategies exhibited some disadvantages such as the high toxicity of QDs, the complex synthesis and purification processes of conjugated polyelectrolytes, and the poor photo-stability, water-solubility of organic fluorescent dyes. Thus, it is still challenging to develop fluorescent ALP assays with simplicity, low toxicity, high sensitivity and selectivity.

In this study, we found that the fluorescent quenching capability of CoOOH was disturbed in the presence of AA, resulting in fluorescence recovery of CuNCs. The recovery of fluorescence might ascribe the specific reduction reaction of CoOOH sheets to Co^{2+} ion with AA, which leading to the disappearance of the CoOOH nanosheets. On the other hand, ALP can catalyze the substrate AA2P hydrolysis and dephosphorylation into AA. Then, the ALP activity can be detected indirectly according to the fluorescence recovery. In addition, the strategy is a signal-on assay and can effectively reduce the false positives. As a result, a sensitive and selective fluorescent assay has been reported for the determination of ALP activity by using CuNC-CoOOH probes.

Experimental

Reagents

Alkaline phosphatase (ALP) from bovine intestinal mucosa, ascorbic acid 2-phosphate (AA2P), ascorbic acid (AA), bovine serum albumin (BSA), thrombin, glucose oxidase (GOx), acetylcholinesterase (AChE), lysozyme, peroxidase from horseradish (HRP), trypsin, copper (II) sulfate pentahydrate ($CuSO_4{\cdot}5H_2O$) were obtained from Sigma Aldrich Chemical Co. (St. Louis, MO, USA, http://www.sigmaaldrich.com). Other chemicals (analytical grade) were purchased from Shanghai Sangon Biological Engineering Technology and Services Co., Ltd. (Shanghai, China, http://www.sangon.com). All the solutions were prepared with ultrapure water (>18.2 MΩ·cm) by using a Millipore Milli-Q water purification system (Billerica, MA, USA, http://www.merckmillipore.com).

Apparatus

The fluorescence spectra were measured on a Hitachi F-7000 fluorescence spectrometer (Hitachi Co. Ltd., Japan). The excitation wavelength was set at 335 nm and the fluorescence emission spectra were collected from 360 to 600 nm at room temperature. The excitation and emission slits were both 5.0 nm. UV-vis absorption spectra were carried out with a Hitachi U-3900 spectrophotometer (Hitachi, Japan). X-ray photoelectron spectroscopy (XPS) was performed with a K-Alpha spectrometer. Transmission electron microscopy (TEM) images were obtained from Tecnai G2F20S-TWIN field emission transmission electron microscopy.

Preparation of CuNCs

Bovine serum albumin (BSA) templated CuNCs were synthesized according to our previous reported methods [29, 30]. Typically, 5 mL 15 $mg{\cdot}mL^{-1}$ BSA solutions were mixed with 1 mL 20 mM $CuSO_4$ solution under stirring at room temperature. Then, pH value of the mixture was adjusted to 12 by using 1 M NaOH. After that, the solution color changed from

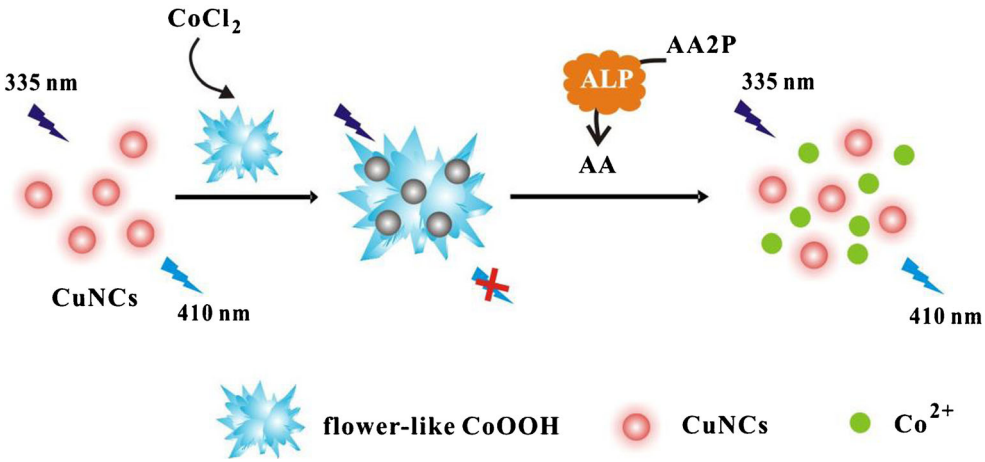

Scheme 1 Schematic illustration of the fluorescent bioassay for ALP activity detection based on CuNC-CoOOH probes

blue to violet. Subsequently, the mixture was incubated at 55 °C under stirring for 2 days. The color changed to light brown. At last, the mixture was dialyzed in ultrapure water to remove excess Cu^{2+}. The final product was stored at 4 °C before use.

Preparation of flower-like CoOOH and CuNC-CoOOH probes

Flower-like CoOOH was synthesized according to the previous methods with minor modifications [5, 7]. Firstly, 100 μL 10 mM $CoCl_2$ and 100 μL 0.8 M NaOH solutions were added to a 1.5 mL microcentrifuge tube. Then, 100 μL 0.2 M NaClO were added into the mixture. Subsequently, 700 μL of ultrapure water was added and treated with ultrasonication for 30 min. After that, the mixture was dialyzed for 8 h in ultrapure water. Finally, the product was collected for further use.

CuNC-CoOOH probes were constructed by the following steps: 50 μL of the prepared CuNCs, 100 μL of different concentrations of $CoCl_2$ and 100 μL 0.8 M NaOH were added to a 1.5 mL microcentrifuge tube. Then, 100 μL 0.2 M NaClO were added. After that, 650 μL of ultrapure water was added and the resulting solutions were ultrasonic treatment for 30 min immediately. Subsequently, the mixture was dialyzed for 8 h in ultrapure water. Finally, CuNC-CoOOH probes were successfully prepared.

Fluorescent detection of AA

In a typical experiment, 50 μL freshly prepared CuNC-CoOOH probe solutions and 10 μL different concentrations of AA were added to 100 μL of bioassay system. After that, the solution was incubated for 2 min at room temperature. Subsequently, the fluorescence intensity was recorded immediately. The excitation wavelength was set at 335 nm and the fluorescence emission spectra were collected from 360 to 600 nm at room temperature. The excitation and emission slits were both 5.0 nm.

Fluorescent assay of ALP activity

In the assay of ALP activity, 5 μL of ALP and 5 μL 10 mM AA2P were added into 10 μL of 20 mM Tris-HCl solutions (pH 7.5, 2 mM $MgCl_2$). The above solution was incubated for 30 min at 37 °C. Subsequently, 50 μL freshly prepared CuNC-CoOOH probes and 30 μL of ultrapure water were added. The

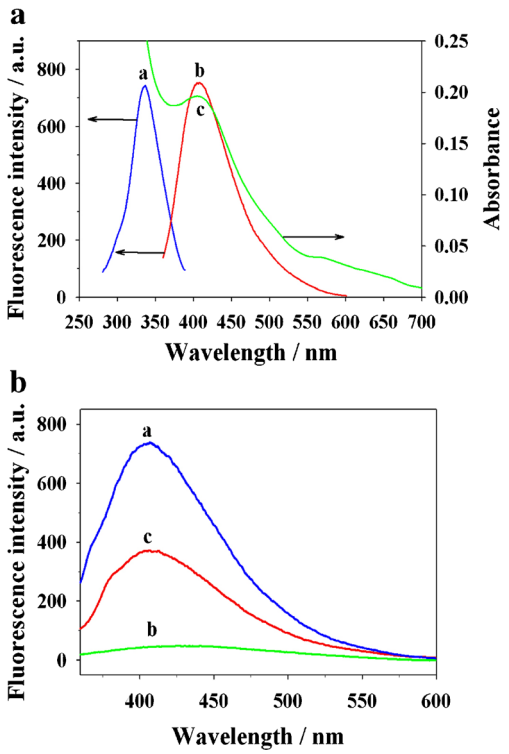

Fig. 1 **a** Fluorescence excitation (*a*) and emission (*b*) spectrum of the CuNCs, and UV-vis absorption spectrum of CoOOH solutions (*c*). **b** Fluorescence spectra of free CuNCs (*a*), CuNC-CoOOH probes (*b*), and CuNC-CoOOH probes with AA (*c*). The excitation wavelength is set at 335 nm

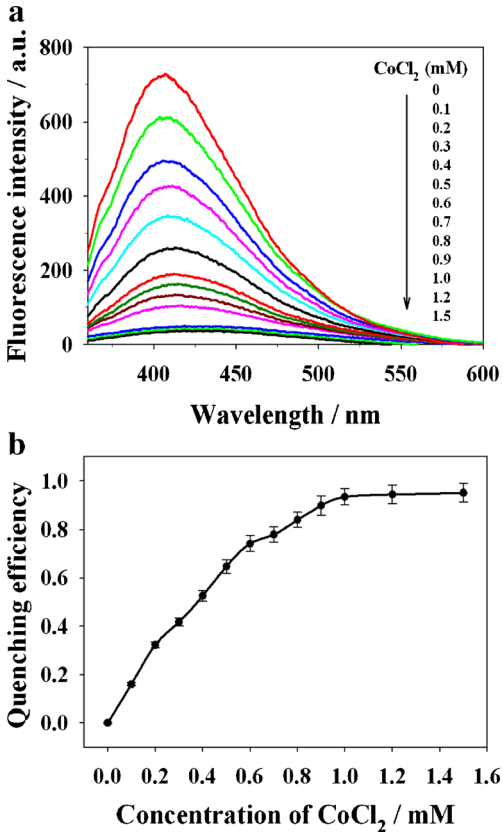

Fig. 2 **a** Fluorescence spectra of CuNC-CoOOH probes formed at a series of different $CoCl_2$ concentrations. **b** Relationship between the fluorescence quenching efficiency and the $CoCl_2$ concentrations

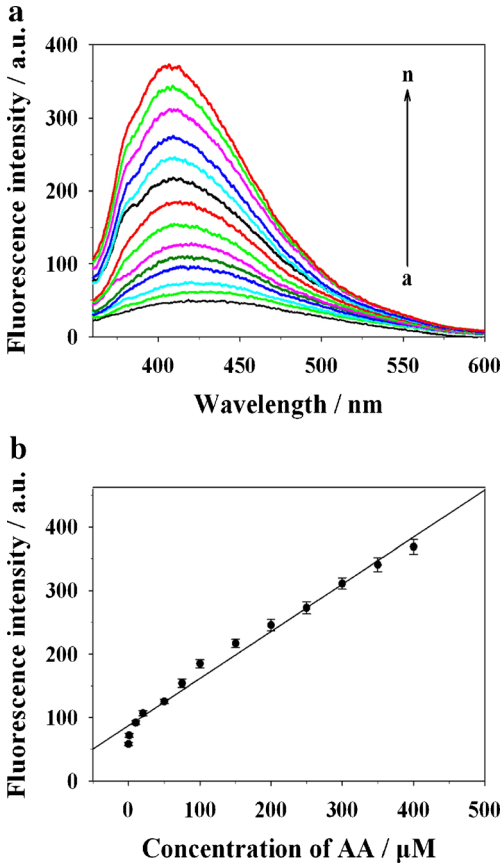

Fig. 3 **a** Fluorescence spectra of CuNC-CoOOH probes in the presence of increasing AA concentrations, the curves from a to n, the concentration of AA are 0, 0.1, 1, 10, 20, 50, 75, 100, 150, 200, 250, 300, 350, 400 μM, respectively. **b** The calibration curve between the fluorescence intensity and the AA concentration. The error bars are the standard deviation of three repetitive measurements

spectrum was measured immediately with the excitation wavelength of 335 nm, after being incubated at room temperature for 5 min.

Results and discussion

Design principle of the fluorescent method for ALP assay

The design principle of the fluorescence bioassay is shown in Scheme 1. CoOOH sheets are prepared through the oxidation of $CoCl_2$ by NaClO in NaOH with ultrasonic treatment. CuNC-CoOOH nanoprobes are constructed by on-line synthesis of CoOOH sheets in CuNC solutions. When nanoprobes are formed, the fluorescence signal of CuNCs can be strongly quenched by CoOOH sheets, due to the large spectral overlapping between the absorption spectrum of CoOOH and the emission spectrum of CuNCs. However, fluorescence recovers in the presence of AA, owning to the AA-mediated specific reduction of the CoOOH to Co^{2+}, combined with the destruction of the CoOOH sheets. Therefore, AA contents can be detected through the fluorescence change of bioassay system. In addition, ALP can catalyze the substrate AA2P hydrolysis and dephosphorylation into AA, which trigger the specific redox reaction of reduced CoOOH into Co^{2+}. Thus, the ALP activity can also be detected indirectly by the amount of enzymatically generated AA according to the fluorescence response.

Characterization of flower-like CoOOH and CuNC-CoOOH probes

The morphology of CoOOH nanomaterials are firstly characterized by SEM images and TEM images. Form Fig. S1A, it is clearly observed that CoOOH sheets are irregular layered structure and assembled to form the flowers-like nanostructure. Fig. S1B displays the TEM image of the flower-like CoOOH. It is seen that CoOOH sheets aggregated together and formed a flowers-like nanostructure, which is the same as the above SEM results. These results confirmed that the flower-like CoOOH had large specific surface areas, which providing an excellent platform for trace determination of AA. As a result, the sensitivity of the assay system is

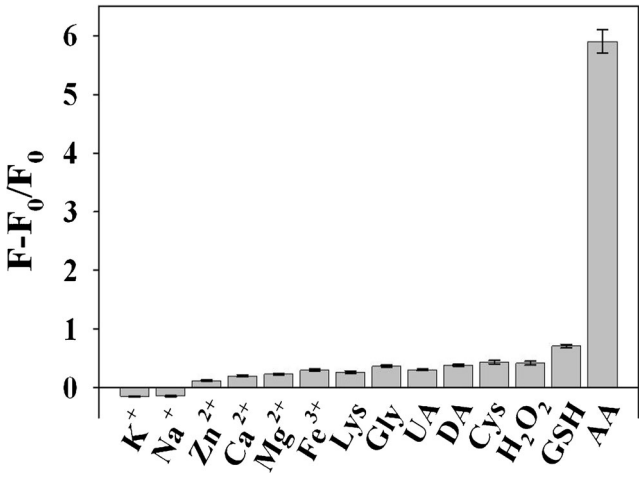

Fig. 4 The selectivity of CuNC-CoOOH probes for AA assay. Where, F_0 and F are the fluorescence intensity in the absence and presence of 400 μM AA, GSH, Cys, H_2O_2 and 4.0 mM other interfering species, respectively

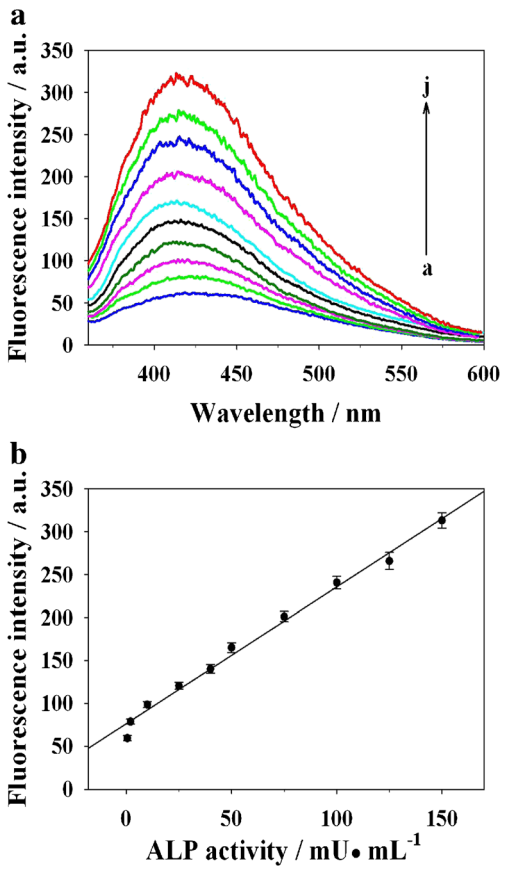

Fig. 5 **a** Fluorescence spectra of bioassay system in the presence of increasing ALP activity, the curves from a to j, the ALP activity are 0.5, 2, 10, 25, 40, 50, 75, 100, 125, 150 mU·mL^{-1}, respectively. **b** The calibration curve between the fluorescence intensity at excitation/emission wavelengths of 335/410 nm and the ALP activity. The error bars are the standard deviation of three repetitive measurements

improved. From Fig. S1C, it is observed that the size of CuNCs is approximately spherical in shape and less than 5 nm in diameter. As shown in Fig. S1D, the CuNCs are interspersed on the surface of the CoOOH sheets. The UV-vis absorption spectrums of $CoCl_2$ and CoOOH sheets are showed in Fig. S1E. It can be observed that $CoCl_2$ possess a strong absorption peak at 510 nm. However, when the flower-like CoOOH is formed, the absorption peak is blue-shifted to 410 nm, which is the same as the reported characteristic absorption spectrum of CoOOH sheets. Figure S1F shows the X-ray photoelectron spectroscopy (XPS) of CuNCs and CuNC-CoOOH probes. From curve a of Fig. S1F, CuNCs possess four elements, Cu, C, N, and O. Besides, two obvious Co 2p peaks are observed from the spectra of CuNC-CoOOH probes (shown in curve b of Fig. S1F and Fig. S1G), which demonstrate the successful preparation of CuNC-CoOOH probes.

Evaluation of fluorescence assay for AA detection

To further evaluate the feasibility of fluorescent assay of AA, the fluorescence response of CuNCs is studied on different experimental conditions. From Fig. 1a, it is found that a strong emission peak at 410 nm can be observed with the excitation wavelength of 335 nm. The fluorescence quantum yield of CuNCs is 15.2%. Importantly, the fluorescence intensity of CuNCs is no obviously changed after stored at 4 °C for 2 months. Furthermore, it is worth noting that absorption spectra flower-like CoOOH (curve c of Fig. 1a) exhibit a large overlap with the emission spectrum of CuNCs (curve b of Fig. 1a). Therefore, the efficient fluorescence quenching occurs by fluorescence resonance energy transfer between CuNCs and CoOOH. Figure 1b displays the over 90% fluorescence signal of CuNCs is strongly reduced when CoOOH is formed (curve b). Interesting, the fluorescence intensity is recovered by 51.5% when the system present 400 μM AA (curve c of Fig. 1b). The enhancement of fluorescence intensity is mainly attributed to the reduction of CoOOH to Co^{2+} ions by AA (shown in Scheme S1), leading to the disappearance of the CoOOH. Due to the separation of CoOOH from CuNCs, the fluorescence intensity recovers.

Optimization of CuNC-CoOOH probes

Since CoOOH is formed by reducing $CoCl_2$ in the presence of NaOH and NaClO, the effect of the $CoCl_2$ concentration on the fluorescent bioassay system is investigated. Figure 2a displays that the fluorescence signal of CuNCs is reduced obviously when the $CoCl_2$ concentrations increase from 0 to 1.5 mM. Nearly 94% fluorescence is decreased when 1.0 mM $CoCl_2$ solution is added. From Fig. 2b, it is found that the quenching efficiency (defined as $(F_0 - F)/F_0$) of CoOOH raises gradually along with the increasing concentrations of the $CoCl_2$. While the concentration of $CoCl_2$ reachs to

Table 1 Comparison of various analytical methods for ALP determination

Analytical methods	Determination range ($mU \cdot mL^{-1}$)	Limit of detection ($mU \cdot mL^{-1}$)	References
T7 exonuclease mediated signal amplification based electrochemical assay	0.1–50	0.1	[34]
Fluorescent carbon dots	2.5–40	1	[35]
Fluorescent Cu nanoparticles	0.3–7.5	0.3	[36]
Graphene oxide and λ exonuclease based fluorescent assay	3–27	0.19	[37]
Carbon dots and MnO_2 nanosheets based fluorescent assay	1–100	0.4	[38]
Cu nanoclusters-CoOOH based fluorescent probes	0.5–150	0.1	this work

1.0 mM, the quenching efficiency has not obviously changed. Thus, 1.0 mM $CoCl_2$ is used in the subsequent experiments.

Optimization of method

The following parameters were optimized: stability of the CuNCs-CoOOH probes and incubated time of ALP. Respective data and Figures are given in the Electronic Supporting Material. It was found that CuNC-CoOOH probes were relatively stable at 20 to 40 °C, pH 6.5 to 8.5, and in different media (Fig. S2). Thirty minutes of incubated time of ALP were found to give best results (Fig. S3).

Fluorescent assay of AA

It was found that the redox reaction between AA and CoOOH was accomplished within 2 min at room temperature, indicating a rapid decomposition of CoOOH by AA. Figure 3a shows the typical fluorescence spectra of CuNC-CoOOH probes in the presence of different concentrations of AA. From curve a to n, it can be seen the fluorescence intensity increased while the AA concentration ranging from 0 μM to 400 μM. The fluorescence recovery is mainly ascribed to the AA-mediated reduction reaction of CoOOH to Co^{2+}, which contributed to the decomposition of CoOOH and the releasing of CuNCs. Figure 3b indicates a good linear relationship between fluorescence intensity and AA concentration (from 0.1 to 400 μM, R = 0.9904). The limit of detection is calculated to be 20 nM. The performance of the assay is compared with literature reports. From Table S1, it can be seen our method exhibits a broader linear range and a lower detection limit than the published methods [31–33]. Additionally, there is not obvious fluorescent response in the presence of other interfering species (including uric acid (UA), dopamine (DA), Cys, H_2O_2 and GSH) (shown in Fig. 4).

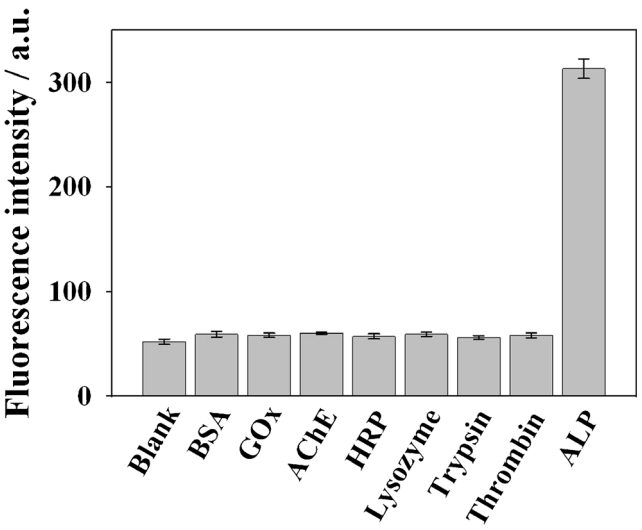

Fig. 6 The selectivity of bioassay system for ALP assay. Each enzyme including ALP, GOx, AChE, HRP, lysozyme, trypsin and thrombin was 150 $mU \cdot mL^{-1}$, the concentrations of BSA was 1 $mg \cdot mL^{-1}$, respectively. The error bars are the standard deviation of three repetitive measurements

Fluorescent method for ALP activity assay

Furthermore, ALP possesses the capability of catalyzing the hydrolysis of AA2P into AA. Therefore, the ALP activity can be detected indirectly according to the fluorescence recovery. The substrate AA2P has no significant reduction capacity and no obvious effect on the fluorescence intensity of CuNC-CoOOH probes. Under the optimized experimental condition, the effect of ALP activity on the fluorescence intensity was recorded in Fig. 5a. When ALP activity increases from 0.5 to 150 $mU \cdot mL^{-1}$ (from curve a to j), the fluorescence intensity rapidly increases. As shown in Fig. 5b, there is a linear correlation between fluorescence intensity and ALP activity (ranging from 0.5 to 150 $mU \cdot mL^{-1}$). The limit of detection is estimated to be 0.1 $mU \cdot mL^{-1}$. The performances of the detection of ALP activity are compared with previously reported methods and listed in Table 1. It is observed that our method is superior to other reported methods with better or comparable detection limit and linear range [34–38].

The selectivity of the bioassay was evaluated by investigating the fluorescence change of other non-specific proteins/enzymes including glucose oxidase (GOx),

acetylcholinesterase (AChE), peroxidase from horseradish (HRP), bovine serum albumin (BSA), lysozyme, trypsin, and thrombin. As shown in Fig. 6, it is obviously seen that the fluorescence intensity of other interfering proteins were little higher than that of the blank experiment (without ALP). The results indicated that this turn-on fluorescent bioassay exhibited a high selectivity toward ALP.

The practical application of the bioassay in real samples was tested by detecting ALP activity in 100-fold diluted human serum samples. As given in Table S2, the relative standard deviations (RSD) are from 2.95% to 4.12% (n = 3) and the recoveries are ranging from 96.7 to 103.0%, indicating the potential of this method for applications in complicated biological samples.

Conclusions

In summary, a fluorescent assay has been reported for ALP activity detection by the AA-decomposited CoOOH-CuNC probes. This strategy is based on the reduction reaction of CoOOH to Co^{2+} ions by AA, which resulting in the decomposition of the CoOOH and the releasing of CuNCs. The assay displays good performance towards determination of ALP activity. So the strategy may find wide applications in drugs screening and early biological and clinical diagnostics. Compared to other fluorescence methods for ALP activity assay, CuNC-CoOOH probes possess good stability and CuNCs have the advantages of strong fluorescence intensity. However, it is a little time consuming to purify the CuNCs.

Acknowledgements This work was financially supported by National Natural Science Foundation of China (No. U1704153, 21305119), Plan for Young Excellent Teachers in Universities of Henan Province (No. 2017GGJS), Nanhu Scholars Program for Young Scholars of XYNU, Plan for Scientific Innovation Talent of Henan Province (No. 2017JR0016), the Science & Technology Innovation Talents in Universities of Henan Province (No. 16HASTIT004).

Compliance with ethical standards The authors declare that they have no competing interests.

References

1. Yuan J, Cen Y, Kong XJ, Wu S, Liu CL, Yu RQ, Chu X (2015) MnO_2-nanosheet-modified upconversion nanosystem for sensitive turn-on fluorescence detection of H_2O_2 and glucose in blood. ACS Appl Mater Interfaces 7:10548–10555
2. Li N, Li YH, Han YY, Pan W, Zhang TT, Tang B (2014) A highly selective and instantaneous nanoprobe for detection and imaging of ascorbic acid in living cells and in vivo. Anal Chem 86:3924–3930
3. Li LB, Wang C, Liu KY, Wang YH, Liu K, Lin YQ (2015) Hexagonal cobalt oxyhydroxide-carbon dots hybridized surface: high sensitive fluorescence turn-on probe for monitoring of ascorbic acid in rat brain following brain ischemia. Anal Chem 87:3404–3411
4. Li GL, Kong WH, Zhao M, Lu SM, Gong PW, Chen G, Xia L, Wang H, You JM, Wu YN (2016) A fluorescence resonance energy transfer (FRET) based "Turn-On" nanofluorescence sensor using a nitrogen-doped carbon dot-hexagonal cobalt oxyhydroxide nanosheet architecture and application to α-glucosidase inhibitor screening. Biosens Bioelectron 79:728–735
5. Cen Y, Tang J, Kong XJ, Wu S, Yuan J, Yu RQ, Chu X (2015) A cobalt oxyhydroxide-modified upconversion nanosystem for sensitive fluorescence sensing of ascorbic acid in human plasma. Nanoscale 7:13951–13957
6. Meng HM, Zhang XB, Yang C, Kuai HL, Mao GJ, Gong L, Zhang WH, Feng SL, Chang JB (2016) Efficient two-photon fluorescence nanoprobe for turn-on detection and imaging of ascorbic acid in living cells and tissues. Anal Chem 88:6057–6063
7. Cen Y, Yang Y, Yu RQ, Chen TT, Chu X (2016) A cobalt oxyhydroxide nanoflake-based nanoprobe for the sensitive fluorescence detection of T4 polynucleotide kinase activity and inhibition. Nanoscale 8:8202–8209
8. Yang Y, Cen Y, Deng WJ, Yu RQ, Chen TT, Chu X (2016) An aptasensor based on cobalt oxyhydroxide nanosheets for the detection of thrombin. Anal Methods 8:7199–7203
9. Chang YQ, Zhang Z, Liu HQ, Wang N, Tang JL (2016) Cobalt oxyhydroxide nanoflake based fluorescence sensing platform for label-free detection of DNA. Analyst 141:4719–4724
10. Coleman JE (2003) Structure and mechanism of alkaline phosphatase. Annu Rev Biophys Biomol Struct 21:441–483
11. Hausamen TU, Helger R, Rick W, Gross W (1967) Optimal conditions for the determination of serum alkaline phosphatase by a new kinetic method. Clin Chim Acta 15:241–245
12. Chen L, Li X, Zheng Z, Lu X, Lin M, Pan C, Liu J (2014) A novel ATP7B gene mutation in a liver failure patient with normal ceruloplasmin and low serum alkaline phosphatase. Gene 538:204–206
13. Christenson RH (1998) Biochemical markers of bone metabolism: an overview. Clin Biochem 30:573–593
14. Ooi K, Shiraki K, Morishita Y, Nobori T (2007) High-molecular intestinal alkaline phosphatase in chronic liver diseases. J Clin Lab Anal 21:133–139
15. Wolf PL (1994) Clinical significance of serum high-molecular-mass alkaline phosphatase, alkaline phosphatase-lipoprotein-X complex, and intestinal variant alkaline phosphatase. J Clin Lab Anal 8:172–176
16. Yang J, Zheng L, Wang Y, Li W, Zhang J, Gu J, Fu Y (2016) Guanine-rich DNA-based peroxidase mimetics for colorimetric assays of alkaline phosphatase. Biosens Bioelectron 77:549–556
17. Hu Q, He MH, Mei YQ, Feng WJ, Jing S, Kong JM, Zhang XJ (2017) Sensitive and selective colorimetric assay of alkaline phosphatase activity with Cu(II)-phenanthroline complex. Talanta 163: 146–152
18. Jiang H, Wang X (2012) Alkaline phosphatase-responsive anodic electrochemiluminescence of CdSe nanoparticles. Anal Chem 84: 6986–6993
19. Ingram A, Moore BD, Graham D (2009) Simultaneous detection of alkaline phosphatase and beta-galactosidase activity using SERRS. Bioorg Med Chem Lett 19:1569–1571
20. Shen CC, Li XZ, Rasooly A, Guo LY, Zhang KN, Yang MH (2016) A single electrochemical biosensor for detecting the activity and inhibition of both protein kinase and alkaline phosphatase based on phosphate ions induced deposition of redox precipitates. Biosens Bioelectron 85:220–225
21. Kong RM, Fu T, Sun NN, Qu FL, Zhang SF, Zhang XB (2013) Pyrophosphate-regulated Zn(2+)-dependent DNAzyme activity: an amplified fluorescence sensing strategy for alkaline phosphatase. Biosens Bioelectron 50:351–355

22. Mao ZQ, Hu L, Zhong C, Zhang H, Liu BF, Liu ZH (2015) A dual-mechanism strategy to design a wide-range pH probe with multi-color fluorescence. Sens Actuators B Chem 219:179–184
23. Jin LY, Dong YM, Wu XM, Cao GX, Wang GL (2015) Versatile and amplified biosensing through enzymatic cascade reaction by coupling alkaline phosphatase in situ generation of photoresponsive nanozyme. Anal Chem 87:10429–10436
24. Guo LY, Chen DL, Yang MH (2017) DNA-templated silver nanoclusters for fluorometric determination of the activity and inhibition of alkaline phosphatase. Microchim Acta 184:2165–2170
25. Xiang MH, Liu JW, Li N, Tang H, Yu RQ, Jiang JH (2016) A fluorescent graphitic carbon nitride nanosheet biosensor for highly sensitive, label-free detection of alkaline phosphatase. Nanoscale 8: 4727–4732
26. Jia L, Xu JP, Li D, Pang SP, Fang Y, Song ZG, Ji J (2010) Fluorescence detection of alkaline phosphatase activity with β-cyclodextrin-modified quantum dots. Chem Commun 46:7166–7168
27. Liu Y, Schanze KS (2008) Conjugated polyelectrolyte-based real-time fluorescence assay for alkaline phosphatase with pyrophosphate as substrate. Anal Chem 80:8605–8612
28. Nutiu R, Yu JMY, Li Y (2004) Signaling aptamers for monitoring enzymatic activity and for inhibitor screening. Chem Bio Chem 5: 1139–1144
29. Wang HB, Chen Y, Li Y, Liu YM (2016) A sensitive fluorescence sensor for glutathione detection based on MnO_2 nanosheets-copper nanoclusters composites. RSC Adv 6:79526–79532
30. Wang HB, Chen Y, Li N, Liu YM (2017) A fluorescent glucose bioassay based on the hydrogen peroxide-induced decomposition of a quencher system composed of MnO_2 nanosheets and copper nanoclusters. Microchim Acta 184:515–523
31. Chen J, Ge J, Zhang L, Li ZH, Li JJ, Sun YH, Qu LB (2016) Reduced graphene oxide nanosheets functionalized with poly(styrene sulfonate) as a peroxidase mimetic in a colorimetric assay for ascorbic acid. Microchim Acta 183:1847–1853
32. Rao HB, Ge HW, Lu ZW, Liu W, Chen ZQ, Zhang ZY, Wang XX, Zou P, Wang YY, He H, Zeng XY (2016) Copper nanoclusters as an on-off-on fluorescent probe for ascorbic acid. Microchim Acta 183: 1651–1657
33. Huang S, Qiu HN, Zhu FW, Lu SY, Xiao Q (2015) Graphene quantum dots as on-off-on fluorescent probes for chromium(VI) and ascorbic acid. Microchim Acta 182:1723–1731
34. Zhang LF, Hou T, Li HY, Li F (2015) A highly sensitive homogeneous electrochemical assay for alkaline phosphatase activity based on single molecular beacon-initiated T7 exonuclease-mediated signal amplification. Analyst 140:4030–4036
35. Kang WJ, Ding YY, Zhou H, Liao QY, Yang X, Yang YG, Jiang JS, Yang MH (2015) Monitoring the activity and inhibition of alkaline phosphatase via quenching and restoration of the fluorescence of carbon dots. Microchim Acta 182:1161–1167
36. Zhang LL, Zhao JJ, Duan M, Zhang H, Jiang JH, Yu RQ (2013) Inhibition of dsDNA-templated copper nanoparticles by pyrophosphate as a label-free fluorescent strategy for alkaline phosphatase assay. Anal Chem 85:3797–3801
37. Liu XG, Xing XJ, Li B, Guo YM, Zhang YZ, Yang Y, Zhang LF (2016) Fluorescent assay for alkaline phosphatase activity based on graphene oxide integrating with λ exonuclease. Biosens Bioelectron 81:460–464
38. Qu FL, Pei HM, Kong RM, Zhu SY, Xia L (2017) Novel turn-on fluorescent detection of alkaline phosphatase based on green synthesized carbon dots and MnO_2 nanosheets. Talanta 165:136–142